Polymer Journal (2021) 53:355–362
https://doi.org/10.1038/s41428-020-00432-4

ORIGINAL ARTICLE

Self-healing polyurethane elastomers based on charge-transfer interactions for biomedical applications

Keiichi Imato[1,2] · Hidekazu Nakajima[1] · Ryota Yamanaka[1] · Naoya Takeda[1]

Received: 26 August 2020 / Revised: 21 September 2020 / Accepted: 24 September 2020 / Published online: 22 October 2020

Abstract

One promising application of self-healing polymeric materials is biomedical use. Although charge-transfer (CT) interactions have been employed to construct self-healing polymers as well as other reversible bonds and interactions, their potential for biomedical applications has never been investigated. In this study, we fabricated self-healable and cell-compatible polyurethane elastomers cross-linked by CT complexes between electron-rich pyrene (Py) and electron-deficient naphthalene diimide (NDI) by simply blending two linear polymers with Py or NDI as a repeating unit. The elastomers with different blend ratios self-healed damage over 1 day in mild conditions, including in air and water at 30–100 °C. The mechanical properties of damaged elastomers were almost restored after healing in air at 100 °C, and even in air at 30 °C and in water at 70 °C, healing was also possible to a certain extent. The good cell compatibility of the polyurethane elastomers was demonstrated by culturing two kinds of cells on the thin film substrates.

Introduction

Self-healing polymeric materials can repair damage at the macroscopic and molecular levels by the materials themselves in appropriate conditions, which is enabled mainly by reversible bonds/interactions, i.e., dynamic covalent bonds and supramolecular interactions [1–7], except for in encapsulation and circulation-based engineering systems [8, 9]. The reversible bonds/interactions incorporated in the polymer networks can be cleaved by mechanical stress (damage) in preference to other strong covalent bonds and recombined by external stimuli suitable for each bond/interaction, including heating, light irradiation, and pH change. Self-healing is useful particularly in space development [10] and biomedical applications such as artificial tissues and organs [11–13], where there is little scope for intervention for repair or replacement and long-term reliability is necessary. Previous self-healing polymeric materials are largely classified into two categories, gels and elastomers, with the single exception of hard polymer glass [14]. Most studies on self-healing polymers for biomedical applications, however, have focused on hydrogels to use them as 3D cell culture scaffolds in tissue engineering [11–13]. Although elastomers are available as structural components of artificial tissues and organs and coatings on them, in which hydrogels cannot be substitutes, to date, self-healable and biocompatible elastomers have rarely been reported [15–24].

Here, we report self-healable and cell-compatible polyurethane elastomers based on the charge-transfer (CT) interaction between electron-rich pyrene (Py) and electron-deficient naphthalene diimide (NDI) as a reversible interaction (Fig. 1) [25]. Unlike hydrogen bonding, one of the most common reversible bonds/interactions in self-healing polymers [26, 27], CT interactions are hardly affected by water molecules and have promise for working under physiological conditions. However, previously developed self-healing polymers based on CT interactions have never been investigated for biomedical applications [28–34]. The reason why we focused on polyurethane is that it has been used in many self-healing polymers [35–39] and

Supplementary information The online version of this article (https://doi.org/10.1038/s41428-020-00432-4) contains supplementary material, which is available to authorized users.

✉ Keiichi Imato
kimato@hiroshima-u.ac.jp

✉ Naoya Takeda
ntakeda@waseda.jp

[1] Department of Life Science and Medical Bioscience, Waseda University (TWIns), 2-2 Wakamatsu-cho, Shinjuku, Tokyo 162-8480, Japan

[2] Department of Applied Chemistry, Hiroshima University, 1-4-1 Kagamiyama, Higashi-Hiroshima 739-8527, Japan

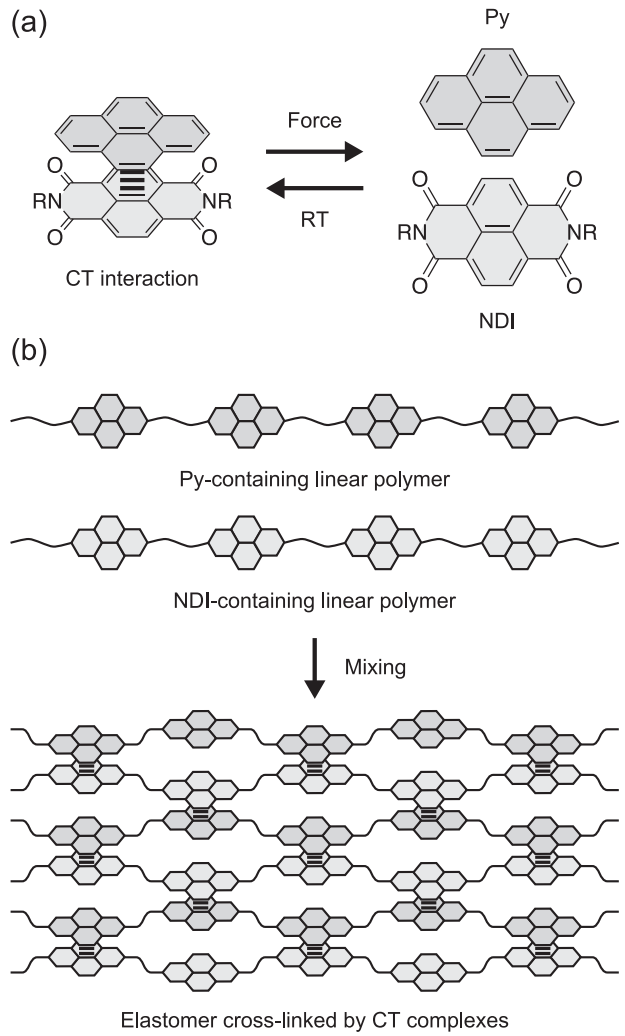

Fig. 1 **a** CT interaction between Py and NDI. **b** Facile fabrication of self-healable elastomers with physical cross-links of CT complexes by simply blending two linear polymers containing Py or NDI as a repeating unit

biomaterials with excellent mechanical properties and good biocompatibility [40, 41]. In this paper, we fabricate elastomers with physical cross-links of CT complexes by simply blending two linear polyurethanes containing either Py or NDI as a repeating unit and evaluate the healing efficiency in various conditions based on their mechanical properties. Cell culture on the elastomer surfaces is also performed to demonstrate cell compatibility.

Experimental procedure

Materials

All solvents and reagents were used as received. **Py-diol** and **NDI-diol**, which have two primary hydroxyl groups at both ends, were synthesized according to our previous paper [25]. Milli-Q water (resistivity > 18 MΩ cm^{-1}) was prepared using a Milli-Q integral water purification system (ZRXQ003JP, Merck Millipore).

Measurements

^{1}H NMR spectroscopic measurements were performed at 25 °C in $CDCl_3$ with tetramethylsilane as the internal standard using a 400-MHz Varian spectrometer. The number-average molecular weights (M_ns) and polydispersity indices (PDIs) of polymers were determined by size exclusion chromatography (SEC) measurements at 40 °C using a JASCO SEC system with a guard column (KF-G 4 A, Shodex), two series-connected columns (KF-806L, Shodex), a UV detector, and a differential refractive index detector. Tetrahydrofuran (THF) was used as the eluent, and polystyrene standards were used to calibrate the SEC system. Fluorescence spectra ($\lambda_{ex} = 340$ nm) were obtained using a SHIMADZU RF-5300PC spectrofluorometer. UV light (365 nm, UVGL-58, UVP) was used to visualize fluorescence intensity changes. Differential scanning calorimetric (DSC) measurements were performed under N_2 at a heating rate of 10 °C min^{-1} using a SHIMADZU DSC-60A Plus. Tensile tests were carried out at a strain rate of 30 mm min^{-1} on rectangular strip specimens (20–30 mm × ca. 3 mm × 0.3–0.6 mm) using a SHIMADZU EZ-S instrument equipped with a 5 N load cell. Static water contact angles were measured at three different positions on a substrate by the sessile drop technique using a drop shape analyzer (DSA100S, Krüss).

Polymer synthesis

Two polyurethanes, **Py-PU** and **NDI-PU**, were synthesized by polyaddition of **Py-diol** or **NDI-diol**, poly(tetramethylene glycol) (PTMG, $M_n = 2000$), and 4,4′-diphenylmethane diisocyanate (MDI) in the presence of a tin catalyst, di-*n*-butyltin dilaurate (DBTDL).

Py-PU

A solution of **Py-diol** (260 mg, 0.742 mmol), PTMG (2.97 g, 1.49 mmol), and MDI (558 mg, 2.23 mmol) in anhydrous *N*, *N*-dimethylformamide (DMF, 16 mL) was prepared under a N_2 atmosphere. A THF solution of 10 vol% DBTDL (1 drop) was added into the mixture, and the mixture was stirred at 70 °C. After 24 h, the mixture was cooled to room temperature and precipitated in MeOH. The precipitate was collected and dried in vacuo at room temperature to give **Py-PU** (3.03 g, 80% yield). ^{1}H NMR (400 MHz, $CDCl_3$): δ (ppm) = 7.93 (m, 4H, Py aromatic), 7.69 (m, 4H, Py aromatic), 7.29 (m, 4H, MDI aromatic), 7.09 (d, $J = 8.0$ Hz, 4H, MDI aromatic), 6.71 (br, NH), 4.47 (t, $J = 6.6$ Hz, 4H,

Py CH_2), 4.37 (t, $J = 6.4$ Hz, 4H, Py CH_2), 3.88 (s, 2H, MDI CH_2), 3.41 (m, 4H, PTMG CH_2), 2.30 (m, 4H, Py CH_2), 1.62 (m, 4H, PTMG CH_2) (Supplementary Fig. S1). $M_n = 38\ 900$ g mol^{-1}, PDI = 2.00.

NDI-PU

A solution of **NDI-diol** (475 mg, 1.07 mmol), PTMG (4.30 g, 2.15 mmol), and MDI (807 mg, 3.22 mmol) in anhydrous DMF (23.6 mL) was prepared under a N_2 atmosphere. A THF solution of 10 vol% DBTDL (1 drop) was added into the mixture, and the mixture was stirred at 70 °C. After 24 h, the mixture was cooled to room temperature and precipitated in MeOH. The precipitate was collected and dried in vacuo at room temperature to give **NDI-PU** (4.65 g, 83% yield). ^{1}H NMR (400 MHz, $CDCl_3$): δ (ppm) = 8.61 (m, 4H, NDI aromatic), 7.29 (m, 4H, MDI aromatic), 7.09 (d, $J = 8.4$ Hz, 4H, MDI aromatic), 6.78 (br, NH), 4.46 (m, 4H, NDI CH_2), 4.23 (m, 4H, NDI CH_2), 3.88 (m, 4H, NDI CH_2 and 2H, MDI CH_2), 3.76 (m, 4H, NDI CH_2), 3.41 (m, 4H, PTMG CH_2), 1.62 (m, 4H, PTMG CH_2) (Supplementary Fig. S2). $M_n = 39\ 000$ g mol^{-1}, PDI = 1.98.

Elastomer preparation

Blend samples of **Py-PU** and **NDI-PU** with different **Py-PU/NDI-PU** (wt/wt) ratios of 1/0, 2/1, 1/1, 1/2, and 0/1 were prepared. Each polymer mixture (960 mg in total) was dissolved in $CHCl_3$ (12 mL), filtered, cast on a Teflon dish, and dried at room temperature in air overnight and in vacuo for 2 h to obtain a thick film (0.3–0.6 mm thickness).

Healing efficiency

The healing efficiency of the blend thick films was evaluated based on the recovery of the elongation at break and maximum stress in tensile tests. A 1 mm nick was made at the center of a rectangular strip specimen (20–30 mm × ca. 3 mm × 0.3–0.6 mm) with a razor blade, and the freshly cut surfaces were immediately made to contact each other and pressed firmly. After healing in air or water at different temperatures (30–100 °C) for different time periods (0–24 h), tensile tests were performed using more than three specimens for each healing condition; three of them were chosen to obtain the average values of the elongation at break and maximum stress.

Cell compatibility

The cell compatibility of the blend elastomer with **Py-PU/NDI-PU** (wt/wt) = 1/1 was evaluated based on cell culture on its thin films. The **Py-PU/NDI-PU** mixture (20 mg) was dissolved in $CHCl_3$ (4 mL), and 360 µL of the solution was spin-coated on cover glass (24 mm × 24 mm, 0.13–0.25 mm thickness, Matsunami Glass) without any surface pretreatment at 3000 rpm for 30 s using a spin coater (ACT-300D, Active). The elastomer-coated glass was dried in air at room temperature for 1 day. Prior to cell seeding, the substrates were exposed to UV light for 15 min at room temperature for sterilization. Bovine aortic endothelial cells (BAECs, P8, Cell Applications) and mouse myoblast (C2C12) cells (P9, RIKEN Cell Bank) were seeded on the elastomer-coated substrates (10% confluence) and cultured at 37 °C with 5% CO_2 in Dulbecco's modified Eagle's medium with high glucose containing 10% fetal bovine serum and 1% penicillin and streptomycin. Cell culture on tissue culture polystyrene (TCPS) dishes was also conducted as a control experiment. The number of adhered cells was calculated by counting the cells collected upon trypsin-ethylenediaminetetraacetic acid treatment. Cell imaging was carried out using a Nikon Eclipse Ti-E/B phase-contrast microscope. For fluorescent imaging, BAECs cultured on the elastomer-coated substrate for 3 days were fixed with 4% paraformaldehyde, and the nuclei and F-actin were fluorescently stained with Hoechst 33342 and Alexa Fluor 568 Phalloidin, respectively. The stained cells were observed using a Nikon Eclipse TE2000-U inverted microscope.

Results and discussion

Polymer synthesis

Two polyurethanes containing either Py or NDI as a repeating unit, **Py-PU** and **NDI-PU**, were synthesized by polyaddition of dihydroxyl Py (**Py-diol**) or NDI (**NDI-diol**), dihydroxyl-terminated PTMG ($M_n = 2000$), and small diisocyanate (MDI) in the presence of a tin catalyst (DBTDL), as shown in Fig. 2 [42–44]. Both polyurethanes have sufficiently large M_ns for mechanical evaluation and remarkably similar M_ns, PDIs, and compositions (Table 1). Compared with the feed ratios, smaller amounts of Py and NDI were incorporated into the polymers (Supplementary Figs. S1 and S2).

Preparation and characterization of elastomers

The cast thick films of **Py-PU** and **NDI-PU** showed brown and orange colors, respectively (Fig. 3a). Blending the polyurethanes produced dark red films, the color of which indicates the formation of CT complexes between Py and NDI units [25, 29, 31, 34]. The CT complexation was also confirmed by the fluorescence spectra in a $CHCl_3$ solution (Fig. 3b) [25, 29, 31]. The intense fluorescence from Py was drastically attenuated in the 1/1 blend solution due to the CT complexation. Fluorescence quenching was clearly observed in the solution by the naked eye under UV light irradiation.

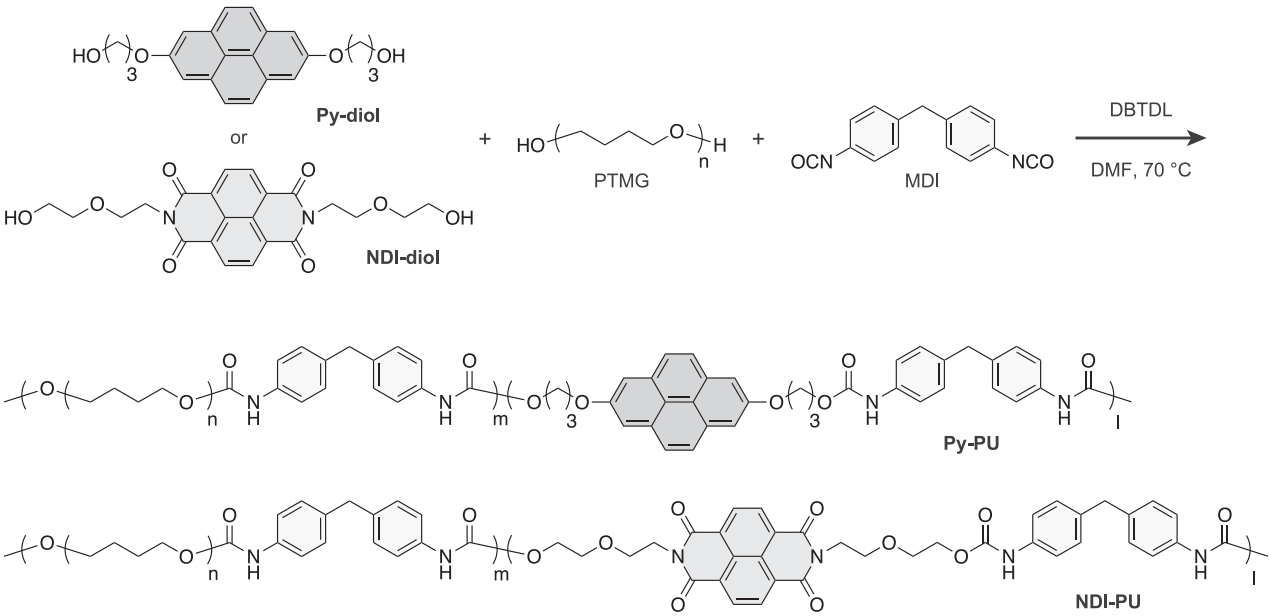

Fig. 2 Synthetic scheme for **Py-PU** and **NDI-PU** by polyaddition

Table 1 M_ns, PDIs, and compositions of **Py-PU** and **NDI-PU**

	Molar ratio[a] (feed ratio)				
	Py or NDI	PTMG	MDI	M_n[b]	PDI[b]
Py-PU	1 (1)	3.4 (2)	4.4 (3)	38 900	2.00
NDI-PU	1 (1)	2.6 (2)	3.6 (3)	39 000	1.98

[a]Calculated from ^{1}H NMR

[b]Determined from SEC

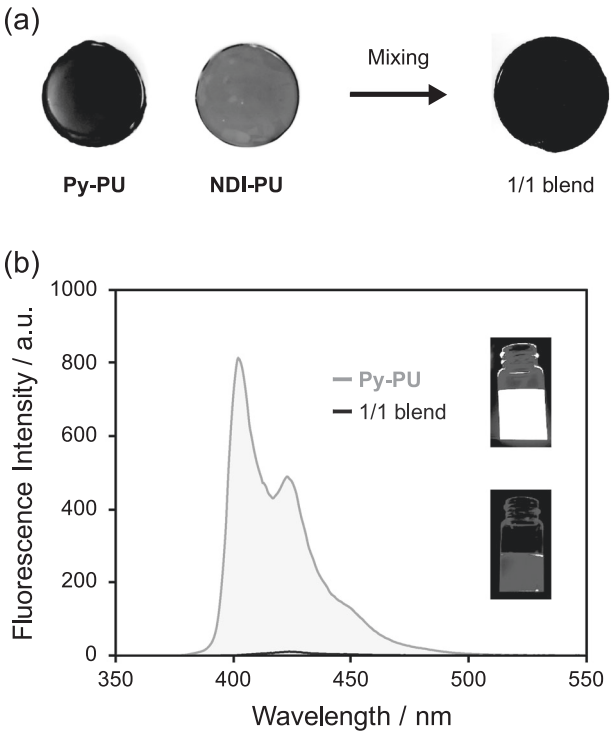

Fig. 3 **a** Photographs of cast thick films of **Py-PU**, **NDI-PU**, and the **Py-PU/NDI-PU** (wt/wt) = 1/1 blend. **b** Fluorescence spectra (λ_{ex} = 340 nm) of **Py-PU** (5 mg mL^{-1}) and the **Py-PU/NDI-PU** (wt/wt) = 1/1 blend (10 mg mL^{-1}) in $CHCl_3$. Inserts are photographs of the **Py-PU** (top) and 1/1 blend (bottom) solutions under UV light (365 nm)

The DSC curve showed that the 1/1 blend has two glass transition temperatures (T_gs) and one melting temperature (T_m), which were similarly observed in **Py-PU** and **NDI-PU** (Fig. 4a). The two T_gs and transparency of the films indicate that the materials are phase-separated at the micro level. The glass transition at approximately −70 °C and melting at ~15 °C originate from the crystalline PTMG [45]. The glass transition at ~90 °C is attributed to the hard domains mainly composed of hard segments with high densities of urethane linkages, which consist of Py, NDI, and MDI and can be statistically generated in the polymerization. As a consequence, the two polyurethanes and their blends are non-crystalline and amorphous elastomers with physical cross-links in the glassy domains: CT complexes between Py and NDI and hydrogen bonds between the urethane linkages at room temperature.

Py-PU resisted high strain and stress, showing good mechanical properties in the tensile tests, whereas **NDI-PU** was extremely weak (Fig. 4b). The difference is probably due to their microstructures but is unrecognizable in the DSC curves. Blending the polyurethanes resulted in tough elastomers with excellent mechanical properties. This is caused by the formation of CT complexes as physical cross-links, which can effectively dissipate energy via

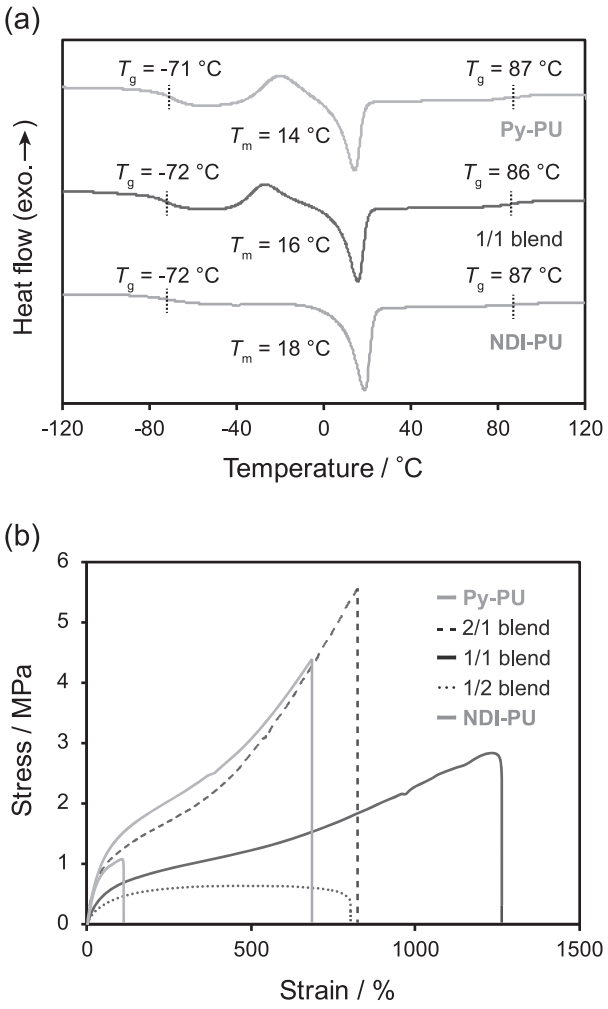

Fig. 4 **a** DSC curves of **Py-PU** (green, top), **NDI-PU** (yellow, bottom), and their 1/1 blend (red, center). **b** Typical stress-strain curves of cast thick films of **Py-PU** (green), **NDI-PU** (yellow), and their 2/1 (red dashed line), 1/1 (red solid line), and 1/2 (red dotted line) blends

dissociation upon mechanical stress [46, 47]. Particularly, the blends with the ratios of **Py-PU**/**NDI-PU** (wt/wt) = 2/1 and 1/1 showed the highest maximum stress and elongation at bleak, respectively, in the tensile tests.

Self-healing

We mainly focused on the 1/1 blend with excellent mechanical properties (elongation at break) and investigated its self-healing behavior (Supplementary Figs. S3 and S4). As the experimental procedure in Fig. 5a shows, a 1 mm nick was made at the center of a rectangular strip film, the freshly cut surfaces were immediately made to contact each other and strongly pressed, and the film was placed in each condition to undergo healing, in which the medium (air or water), temperature (30–100 °C), and time period (0–24 h) were varied. After healing, the specimens were stretched to measure the mechanical properties. The stress-strain curves

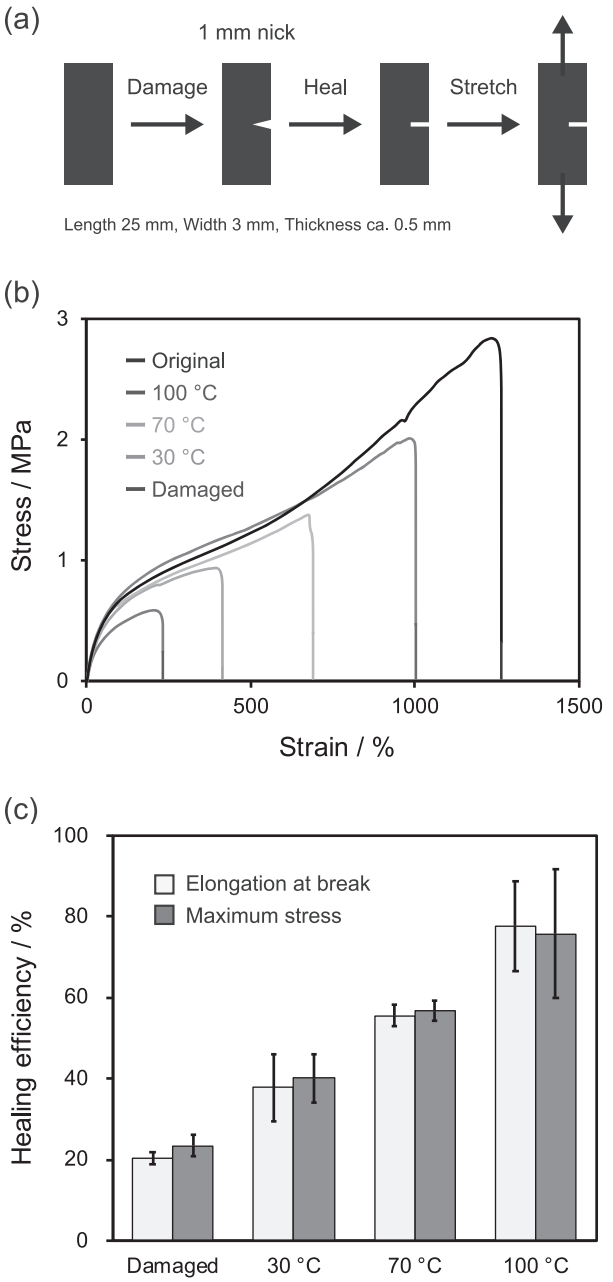

Fig. 5 **a** Illustration of the quantitative evaluation of the healing efficiency by tensile tests. **b**, **c** Temperature effect on the healing behavior of the 1/1 blend elastomer film. **b** Typical stress-strain curves of thick films without (black) and with (blue) a nick and after healing in air at 30 (green), 70 (yellow), and 100 °C (red) for 24 h. **c** Healing efficiency estimated from the elongation at break (white) and maximum stress (gray) in the tensile tests (mean ± SD, $n = 3$)

of the damaged specimens gradually recovered to the intact curve with increasing temperature during healing in air for 24 h (Fig. 5b). The specimens after healing at 30 and 70 °C fractured at the nick in the tensile tests, whereas those after healing at 100 °C broke at random positions similar to the intact specimens, which indicates that the mechanical properties were almost restored. The healing efficiency was

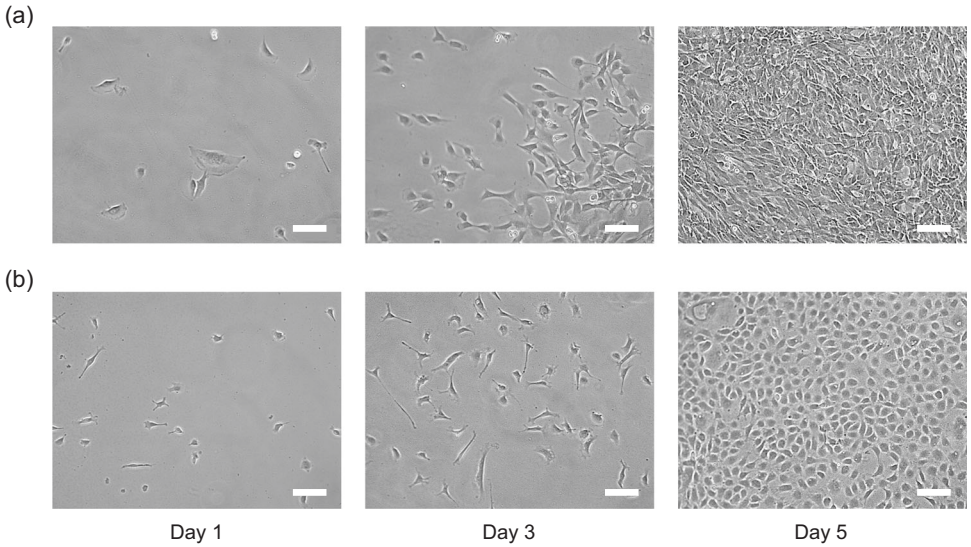

Fig. 6 Phase-contrast microscopic images of **a** C2C12 cells and **b** BAECs cultured on 1/1 blend thin films for 1, 3, or 5 day(s). Scale bars are 100 μm

determined from the recovery of the elongation at break and maximum stress in the curves (Fig. 5c). The healing in air at 30, 70, and 100 °C for 24 h enabled recoveries of nearly 40%, 60%, and 80%, respectively. Even under mild conditions at 30 °C close to body temperature, healing was possible to a certain extent. During the healing processes at all temperatures, including 100 °C, the specimens were not fluid but retained their original shapes at the macroscopic level, although the DSC curves suggest liquefaction of the blends at ~90 °C. This indicates that the physical cross-links, such as CT complexes between Py and NDI and hydrogen bonds between the urethane linkages [45], maintained the polymer network structures. Therefore, we concluded that the blend elastomers healed damage by themselves without melting.

An increase in the time period was also effective for better healing (Supplementary Fig. S5). In addition, such healing was observed in the other blends with **Py-PU/NDI-PU** (wt/wt) = 2/1 and 1/2 ratios (Supplementary Fig. S6). To explore the potential for use in physiological conditions, healing in water was investigated (Supplementary Fig. S7). Although the efficiency was lower than that in air, healing was possible to a certain extent in water. The reason for the lower efficiency is probably that water penetrated into the nick and physically interfered with the healing.

Cell compatibility

For biomedical use of the self-healable blend elastomers, the cell compatibility was evaluated by culturing two kinds of cells, C2C12 cells and BAECs, on the elastomer surfaces. C2C12 cells were selected because of their characteristic as the precursor cells of self-healable muscle tissue and strong adhesion property, while BAECs were employed to examine the behavior of weak adhesion cells. Thin films of the 1/1 blend elastomer were fabricated on glass substrates by spin-coating (thickness < 100 nm) [48], and the cells were seeded on the surfaces. Both cells adhered to the substrates, extended, and proliferated well (Fig. 6). One possible reason for the strong adhesion is the hydrophobicity of the surfaces, which showed a water contact angle of 80.2° ± 3.8°. It is well known that most adhesive cells and cell-adhesive proteins prefer hydrophobic surfaces with water contact angles of ~70–80° [49]. Nuclei and F-actin were fluorescently stained in BAECs cultured on the substrate for 3 days to investigate the cell adhesion in detail (Fig. 7). The fluorescence microscopic image showed that the BAECs remarkably formed actin stress fibers, indicating strong adhesion on the surface with metabolic activity. Furthermore, the doubling time of BAECs was 16.7 h, which was comparable to that on TCPS (15.8 h). From these results, we concluded that the blend elastomers have good cell compatibility, as expected.

Interestingly, C2C12 cells did not adhere to the cast thick film of the 1/1 blend (thickness = 0.3–0.6 mm, Supplementary Fig. S8). Because the moduli of culture scaffolds strongly affect cell adhesion [50], the thick film without a stiff glass substrate would be soft for C2C12 cells. This result potentially suggests that if the blend elastomers are employed as coatings on artificial tissues and organs, we can select whether the surfaces are cell-adhesive or not for the intended use by tuning the thickness.

Conclusion

In this study, we fabricated self-healable and cell-compatible elastomers cross-linked by reversible CT complexes between electron-rich Py and electron-deficient NDI

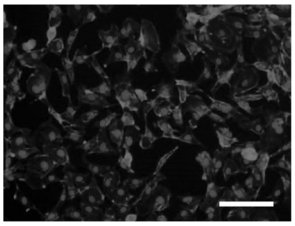

Fig. 7 Microscopic image of fluorescently stained BAEC nuclei (blue) and F-actin (red) on a 1/1 blend thin film at 3 days of culture. The scale bar is 100 μm

units by simply blending two linear polyurethanes with either Py or NDI as a repeating unit but with remarkably similar chemical structures (M_ns, PDIs, and compositions). The blend elastomers with different Py/NDI ratios healed damage by themselves over 1 day in mild conditions such as in air and water at 30–100 °C. The healing efficiency was quantitatively evaluated based on the recovery of mechanical properties measured by tensile tests. Nearly 80% recovery was possible without liquefaction after healing in air at 100 °C, while healing to a certain extent was also observed in air at 30 °C and in water at 70 °C. The good proliferation of C2C12 cells and BAECs on their thin film substrates demonstrated the cell compatibility of the elastomers. This study investigated the potential of self-healable elastomers based on CT interactions for biomedical use for the first time despite recent intense research on such elastomers. We believe that the findings obtained in this study will contribute to the development of self-healable polymeric biomaterials based on reversible bonds/interactions.

Acknowledgements This work was supported by JSPS KAKENHI (Grant No. 16H07292 and 19K15623, KI), MEXT LEADER (Grant No. A6501, KI), and the Izumi Science and Technology Foundation (Grant No. H29-J-113, KI). A research grant from the Mitsubishi Materials–Faculty of Science and Engineering, Waseda University (2016, 2018) and a Grant for Young Scientists Encouragement from the Waseda Research Institute for Science and Engineering–JXTG Energy (2017) are also acknowledged for financial support.

Compliance with ethical standards

Conflict of interest The authors declare that they have no conflict of interest.

Publisher's note Springer Nature remains neutral with regard to jurisdictional claims in published maps and institutional affiliations.

References

1. Herbst F, Döhler D, Michael P, Binder WH. Self-healing polymers via supramolecular forces. Macromol Rapid Commun. 2013;34:203–20.
2. Harada A, Takashima Y, Nakahata M. Supramolecular polymeric materials via cyclodextrin–guest interactions. Acc Chem Res. 2014;47:2128–40.
3. Roy N, Bruchmann B, Lehn J-M. DYNAMERS: dynamic polymers as self-healing materials. Chem Soc Rev. 2015;44:3786–807.
4. Yang Y, Ding X, Urban MW. Chemical and physical aspects of self-healing materials. Prog Polym Sci. 2015;49-50:34–59.
5. Imato K, Otsuka H. Dynamic Covalent Chemistry: Principles, Reactions and Applications. In: Zhang W, Jin Y, editors. Hoboken, NJ, USA: John Wiley & Sons; 2017. p. 359–87.
6. Imato K, Otsuka H. Reorganizable and stimuli-responsive polymers based on dynamic carbon-carbon linkages in diarylbibenzofuranones. Polymer. 2018;137:395–413.
7. Dahlke J, Zechel S, Hager MD, Schubert US. How to design a self-healing polymer: general concepts of dynamic covalent bonds and their application for intrinsic healable materials. Adv Mater Interfaces. 2018;50:1800051.
8. Diesendruck CE, Sottos NR, Moore JS, White SR. Biomimetic self-healing. Angew Chem Int Ed. 2015;54:10428–47.
9. Patrick JF, Robb MJ, Sottos NR, Moore JS, White SR. Polymers with autonomous life-cycle control. Nature. 2016;540:363–70.
10. Levchenko I, Bazaka K, Belmonte T, Keidar M, Xu S. Advanced materials for next-generation spacecraft. Adv Mater. 2018;41:1802201.
11. Tu Y, Chen N, Li C, Liu H, Zhu R, Chen S, et al. Advances in injectable self-healing biomedical hydrogels. Acta Biomater. 2019;90:1–20.
12. Talebian S, Mehrali M, Taebnia N, Pennisi CP, Kadumudi FB, Foroughi J, et al. Self-healing hydrogels: the next paradigm shift in tissue engineering? Adv Sci. 2019;6:1801664.
13. Uman S, Dhand A, Burdick JA. Recent advances in shear-thinning and self-healing hydrogels for biomedical applications. J Appl Polym Sci. 2019;336:48668–20.
14. Yanagisawa Y, Nan Y, Okuro K, Aida T. Mechanically robust, readily repairable polymers via tailored noncovalent cross-linking. Science. 2018;359:72–76.
15. Zhao J, Xu R, Luo G, Wu J, Xia H. Self-healing poly(siloxane-urethane) elastomers with remoldability, shape memory and biocompatibility. Polym Chem. 2016;7:7278–86.
16. Zhao J, Xu R, Luo G, Wu J, Xia H. A self-healing, re-moldable and biocompatible crosslinked polysiloxane elastomer. J Mater Chem B. 2016;4:982–9.
17. Daemi H, Rajabi-Zeleti S, Sardon H, Barikani M, Khademhosseini A, Baharvand H. A robust super-tough biodegradable elastomer engineered by supramolecular ionic interactions. Biomaterials. 2016;84:54–63.
18. Chen S, Bi X, Sun L, Gao J, Huang P, Fan X, et al. Poly(sebacoyl diglyceride) cross-linked by dynamic hydrogen bonds: a self-healing and functionalizable thermoplastic bioelastomer. ACS Appl Mater Interfaces. 2016;8:20591–9.
19. Wu Y, Wang L, Zhao X, Hou Sen, Guo B, Ma PX. Self-healing supramolecular bioelastomers with shape memory property as a multifunctional platform for biomedical applications via modular assembly. Biomaterials. 2016;104:18–31.
20. Liu L, Zhu L, Zhang L. A solvent-resistant and biocompatible self-healing supramolecular elastomer with tunable mechanical properties. Macromol Chem Phys. 2017;219:1700409–7.
21. Tallia F, Russo L, Li S, Orrin ALH, Shi X, Chen S, et al. Bouncing and 3D printable hybrids with self-healing properties. Mater Horiz. 2018;5:849–60.
22. Li F, Ye Q, Gao Q, Chen H, Shi SQ, Zhou W, et al. Facile fabrication of self-healable and antibacterial soy protein-based films with high mechanical strength. ACS Appl Mater Interfaces. 2019;11:16107–16.
23. Liu J, Duan W, Song J, Guo X, Wang Z, Shi X, et al. Self-healing hyper-cross-linked metal–organic polyhedra (HCMOPs) membranes with antimicrobial activity and highly selective separation properties. J Am Chem Soc. 2019;141:12064–70.

24. Zeimaran E, Pourshahrestani S, Kadri NA, Kong D, Shirazi SFS, Naveen SV, et al. Self-healing polyester urethane supramolecular elastomers reinforced with cellulose nanocrystals for biomedical applications. Macromol Biosci. 2019;19:1900176–12.
25. Imato K, Yamanaka R, Nakajima H, Takeda N. Fluorescent supramolecular mechanophores based on charge-transfer interactions. Chem Commun. 2020;56:7937–40.
26. Cordier P, Tournilhac F, Soulié-Ziakovic C, Leibler L. Self-healing and thermoreversible rubber from supramolecular assembly. Nature. 2008;451:977–80.
27. Tamate R, Hashimoto K, Horii T, Hirasawa M, Li X, Shibayama M, et al. Self-healing micellar ion gels based on multiple hydrogen bonding. Adv Mater. 2018;30:1802792–7.
28. Burattini S, Colquhoun HM, Fox JD, Friedmann D, Greenland BW, Harris PJF, et al. A self-repairing, supramolecular polymer system: healability as a consequence of donor–acceptor π–π stacking interactions. Chem Commun. 2009;6717–9.
29. Burattini S, Greenland BW, Merino DH, Weng W, Seppala J, Colquhoun HM, et al. A healable supramolecular polymer blend based on aromatic π−π stacking and hydrogen-bonding interactions. J Am Chem Soc. 2010;132:12051–8.
30. Fox J, Wie JJ, Greenland BW, Burattini S, Hayes W, Colquhoun HM, et al. High-strength, healable, supramolecular polymer nanocomposites. J Am Chem Soc. 2012;134:5362–8.
31. Hart LR, Harries JL, Greenland BW, Colquhoun HM, Hayes W. Supramolecular approach to new inkjet printing inks. ACS Appl Mater Interfaces. 2015;7:8906–14.
32. Hart LR, Nguyen NA, Harries JL, Mackay ME, Colquhoun HM, Hayes W. Perylene as an electron-rich moiety in healable, complementary π-π stacked, supramolecular polymer systems. Polymer. 2015;69:293–300.
33. Qin J, Lin F, Hubble D, Wang Y, Li Y, Murphy IA, et al. Tuning self-healing properties of stiff, ion-conductive polymers. J Mater Chem A. 2019;7:6773–83.
34. Xiao W-X, Liu D, Fan C-J, Xiao Y, Yang K-K, Wang Y-Z. A high-strength and healable shape memory supramolecular polymer based on pyrene-naphthalene diimide complexes. Polymer. 2020;190:122228.
35. Imato K, Takahara A, Otsuka H. Self-healing of a cross-linked polymer with dynamic covalent linkages at mild temperature and evaluation at macroscopic and molecular levels. Macromolecules. 2015;48:5632–9.
36. Imato K, Natterodt JC, Sapkota J, Goseki R, Weder C, Takahara A, et al. Dynamic covalent diarylbibenzofuranone-modified nanocellulose: mechanochromic behaviour and application in self-healing polymer composites. Polym Chem. 2017;8:2115–22.
37. Kim S-M, Jeon H, Shin S-H, Park S-A, Jegal J, Hwang SY, et al. Superior toughness and fast self-healing at room temperature engineered by transparent elastomers. Adv Mater. 2018;30:1705145–8.
38. Zhang L, Liu Z, Wu X, Guan Q, Chen S, Sun L, et al. A highly efficient self-healing elastomer with unprecedented mechanical properties. Adv Mater. 2019;31:1901402–8.
39. Hornat CC, Urban MW. Entropy and interfacial energy driven self-healable polymers. Nat Commun. 2020;11:1028.
40. Gunatillake PA, Adhikari R, Gadegaard N. Biodegradable synthetic polymers for tissue engineering. Eur Cells Mater. 2003;5:1–16.
41. Teo AJT, Mishra A, Park I, Kim Y-J, Park WT, Yoon YJ. Polymeric biomaterials for medical implants and devices. ACS Biomater Sci Eng. 2016;2:454–72.
42. Imato K, Nishihara M, Kanehara T, Amamoto Y, Takahara A, Otsuka H. Self-healing of chemical gels cross-linked by diarylbibenzofuranone-based trigger-free dynamic covalent bonds at room temperature. Angew Chem Int Ed. 2012;51:1138–42.
43. Imato K, Ohishi T, Nishihara M, Takahara A, Otsuka H. Network reorganization of dynamic covalent polymer gels with exchangeable diarylbibenzofuranone at ambient temperature. J Am Chem Soc. 2014;136:11839–45.
44. Imato K, Irie A, Kosuge T, Ohishi T, Nishihara M, Takahara A, et al. Mechanophores with a reversible radical system and freezing-induced mechanochemistry in polymer solutions and gels. Angew Chem Int Ed. 2015;54:6168–72.
45. Imato K, Kanehara T, Nojima S, Ohishi T, Higaki Y, Takahara A, et al. Repeatable mechanochemical activation of dynamic covalent bonds in thermoplastic elastomers. Chem Commun. 2016;52:10482–5.
46. Sun TL, Kurokawa T, Kuroda S, Ihsan AB, Akasaki T, Sato K, et al. Physical hydrogels composed of polyampholytes demonstrate high toughness and viscoelasticity. Nat Mater. 2013;12:932–7.
47. Nakahata M, Takashima Y, Harada A. Highly flexible, tough, and self-healing supramolecular polymeric materials using host-guest interaction. Macromol Rapid Commun. 2016;37:86–92.
48. He D, Arisaka Y, Masuda K, Yamamoto M, Takeda N. A photoresponsive soft interface reversibly controls wettability and cell adhesion by conformational changes in a spiropyran-conjugated amphiphilic block copolymer. Acta Biomater. 2017;51:101–11.
49. Tamada Y, Yoshito I. Effect of preadsorbed proteins on cell adhesion to polymer surfaces. J Colloid Interface Sci. 1993;155:334–9.
50. Li Y, Xiao Y, Liu C. The Horizon of Materiobiology: A perspective on material-guided cell behaviors and tissue engineering. Chem Rev. 2017;117:4376–421.